

See discussions, stats, and author profiles for this publication at: <https://www.researchgate.net/publication/282052817>

Niche Mimicking for Selection and Enrichment of Liver Cancer Stem Cells by Hyaluronic Acid-Based Multilayer Films

ARTICLE in ACS APPLIED MATERIALS & INTERFACES · SEPTEMBER 2015

Impact Factor: 6.72 · DOI: 10.1021/acsmami.5b04436

READS

12

3 AUTHORS, INCLUDING:



I-Chi Lee

Chang Gung University

22 PUBLICATIONS 240 CITATIONS

[SEE PROFILE](#)

Niche Mimicking for Selection and Enrichment of Liver Cancer Stem Cells by Hyaluronic Acid-Based Multilayer Films

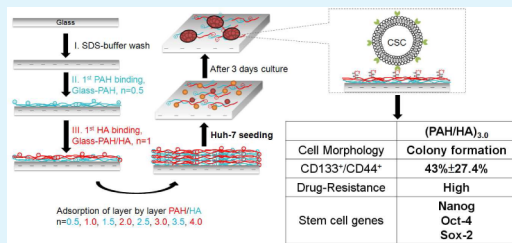
I-Chi Lee,* Chun-Chieh Chuang, and Yu-Chieh Wu

Graduate Institute of Biochemical and Biomedical Engineering, Chang Gung University, No. 259, Wenhua First Road, Guishan District, Taoyuan 33302, Taiwan

Supporting Information

ABSTRACT: Cancer stem cells (CSCs) represent a subpopulation of tumor cells that exhibit capacities for self-renewal, tumor initiation, disease relapse or metastasis, and resistance to chemotherapy and radiotherapy. However, the major obstacle associated with the use of CSCs is the difficulty in their isolation and enrichment. According to recent studies, CSCs share similar properties with normal stem cells, and it has been observed that hyaluronan (HA) plays a key factor in CSCs niches and that HA-mediated CD44 interaction promotes tumor progression. Therefore, HA-based multilayer films were used to fabricate sequential surface properties variation and to mimic CSC niches. A quartz crystal microbalance was used to investigate the layer-by-layer adsorption of PAH/HA multilayer films. Colony formation was observed on a series of poly(allylamine hydrochloride) PAH/HA multilayer films, and cytotoxicity and cell viability were evaluated by MTT, LDH and live/dead assay. It was observed that the cells isolated from $(\text{PAH}/\text{HA})_3$ displayed the best colony formation ability and that the expression of CD133/CD44 double positive cells was up-regulated to approximately 70% after 7 days of culture. Furthermore, the cells isolated from $(\text{PAH}/\text{HA})_3$ displayed higher chemo-resistance than the control group. The stem-cell-related genes expression of selected cells from $(\text{PAH}/\text{HA})_3$ after 7 days of culture was significantly different from that of the control group. In conclusion, this study provides a label-free selection and enrichment system that could serve as a new strategy for the future development of CSC selection and drug evaluation in cancer therapy.

KEYWORDS: cancer stem cells, label-free selection, hyaluronan (HA), CD44, PEM films, drug resistance



INTRODUCTION

It is widely accepted that a subpopulation of cancer cells exhibits stem-cell-like characteristics and is regarded as the cause of tumor formation, recurrence, and failure of chemo- and radiotherapy.^{1–3} The selection, enrichment, and characterization of cancer stem cells (CSCs) could help to develop new therapeutic strategies for targeting CSCs specifically. However, the major obstacle in this regard is the difficulty on isolating CSCs.

Hepatocellular carcinoma (HCC) is one of the world's most aggressive diseases with rising incidence over the past decades.⁴ Previous researchers have reported that liver CSCs could be sorted by surface markers, such as CD133, CD44, CD90, and epithelial cell adhesion molecule (EpCAM).^{5–7} In addition, the side population (SP) method and radio-resistant selection method have also been used to select a small SP fraction that can self-renew, which are possibly CSCs.^{8,9} SP has also been found in cell lines and displays the capacity for self-renewal and chemoresistance.¹⁰ However, these conventional methods require well-defined biomarkers or complicated labeling procedures that are uneconomical and often unreliable.¹¹ These selection methods may also affect culture and enrichment: for example, cells after treatment with radiolabeling may result in residual reagents, mutation, or cell toxicity.^{9,12} In addition, no marker that can be used as a single prognostic

parameter for putative liver CSCs has yet been accepted because of the lack of universally accepted markers of these cells.¹¹ Therefore, the establishment of robust and reliable methods is required for the isolation of liver CSCs.

It is well recognized that stem cell niches provide a particular microenvironment for cells to maintain stem-cell-like characteristics and support CSC self-renewal and simultaneously serve as a physical barrier to protect CSCs from chemotherapeutic agents.^{13,14} The microenvironment or niche surrounding CSCs largely governs their cellular fate, and in this context, the extracellular matrix (ECM) plays an essential role in anchoring CSCs to their niches.¹⁴ The transmembrane glycoprotein hyaluronan (HA) is an important component of stem cell and CSC niches, and HA concentrations are usually higher in malignant tumors.^{15,16} In addition, CD44 is overexpressed in various tumors, including HCC, and has been widely used to sort CSCs.^{15–17} It has been demonstrated that high levels of HA correlate with and actively promote tumor progression.¹⁸ In addition, products degraded from HA can stimulate angiogenesis from tumors.¹⁸ Accumulating evidence shows

Received: May 21, 2015

Accepted: September 17, 2015



ACS Publications

© XXXX American Chemical Society

A

DOI: 10.1021/acsami.5b04436
ACS Appl. Mater. Interfaces XXXX, XXX, XXX–XXX

that HA-CD44 interactions promote tumor-cell-specific behavior such as tumor growth and metastasis.^{16,19}

Accordingly, self-assembled colonies and spheroids have been shown to be important characteristic of stem cells and CSCs. Concurrent studies have also confirmed that colony formation and growth serve as physiologic tumor models^{20–22} and that subpopulations of CSCs sorted from cancer cells can be enriched in spheres when cultured in serum-free medium.^{21,23,24} Our previous study used supported lipid bilayer adsorbed polyelectrolyte multilayer (PEM) films to mimic stem cell niches and regulate colony formation for fetal liver stem cell selection.²⁵ It is well recognized that series of multilayer films provide film growth and a variation in surface properties that may affect cell behavior. By varying the electrolyte composition, assembly conditions, and pH control can regulate the properties of the multilayer films, such as surface charge, roughness, films hydration, surface softness, all of which may alter cell behaviors includes cell adhesion, colony formation, and stem cell differentiation. In addition, the fabrication and alteration of PEM films do not need the complicated instrument and may combine with microfluidic system on the application for drug testing. Based on these reasons, HA was chosen as an ideal suitable material for fabricating multilayer films to mimic CSC niches. In this study, a series of poly(allylamine hydrochloride) PAH/HA multilayer films were fabricated to induce microenvironment variation and to mimic CSC niches for colony formation, label-free cell selection, and enrichment. PEM films with controlled architecture were created by the alternate deposition of PAH and HA on glass slides. Layer-by-layer film growth was confirmed by measurements made using quartz crystal microbalance (QCM). The CSC marker expression and chemo-resistance of these selected colonies on PAH/HA multilayer films were determined. Moreover, it has been shown that certain key regulators such as octamer-binding transcription factor 4 (Oct4), sex-determining region Y box 2 (Sox2), and Nanog of embryonic stem cells are more frequently overexpressed in CSCs in several types of cancers.²⁶ Therefore, stem-cell-like gene expression was also evaluated in this study.

EXPERIMENTAL SECTION

Preparation of PAH/HA Multilayer Films. Layer-by-layer PAH/HA multilayer films were prepared following a procedure described in our previous study, with some modifications.²⁷ First, PAH and HA were dissolved in 10 mM tris(hydroxymethyl) aminomethane buffer with 150 mM NaCl at pH 7.4 at a concentration of 3 mg mL⁻¹, respectively. To deposit the films, glass coverslips were pretreated with 0.01 M sodium dodecyl sulfate (SDS) with 0.12 M HCl at 100 °C, 15 min and then rinsed with deionized water. The glass coverslips were then immersed in a PAH (MW = 65 kDa, Sigma-Aldrich) solution for 10 min at room temperature and then rinsed with 1 mL of Tris-HCl buffer three times, each time for 4 min. The PAH-coated glass slides were then immersed in an HA (MW = 300 kDa, Sigma, St Louis, MO) solution for 10 min and washed as previously described. Finally, the substrates were washed with fresh PBS to remove any uncoupled polyelectrolytes. The layered materials were designated (PAH/HA)_n, where n denotes the number of polyelectrolyte pairs formed by repeating the above-described steps. For instance, n = 0.5 indicates that only PAH was deposited, and n = 1 denotes a PAH/HA pair.

Fabrication of the Multilayer Films Constructs Using a QCM Assay. A QCM assay was performed as described in our previous study.²⁷ A QCM system employing AT-cut quartz crystals, P-chip (Au-2S, ANT Technology Co. Ltd., Taiwan), was used to monitor the growth of PAH/HA multilayers. The crystals were pretreated with O₂

plasma cleaner (Harrick Plasma, PDC-001-HP) and variations in frequency were continuously recorded.

Zeta Potential Measurement. The zeta potential measurement (Anton, Pear-Electro Kinetic Analyzer, Graz, Austria) was applied after PAH/HA multilayer films coating on glass coverslip and then immersed in a stream potential of 10⁻³ M KCl solution with pH 7.4.

Cell Culture Conditions and Morphology Investigation.

Human HCC cell line Huh7 was provided as a gift from Dr. Shen. Cells were cultured in Dulbecco's modified Eagle's medium (DMEM) supplemented with 10% fetal calf serum (Gibco-RBL Life Technologies, Paisley, UK) and antibiotic/antimycotic (Gibco-BRL Life Technologies, Paisley, UK) in a humidified atmosphere composed of 5% CO₂. To examine colony formation, 1 mL of the cell suspension at a concentration of 3 × 10⁴ cells/mL was added to each well for the HA only and PAH/HA multilayer coatings and maintained in a humidified atmosphere composed of 5% CO₂ at 37 °C. Cell morphology and colony formation on different substrates and a TCPS control were observed using a fluorescence microscope equipped with a digital camera (ECLIPSE-TS100, Nikon, USA).

Lactate Dehydrogenase Activity Assay. The cytotoxicity of the PAH/HA multilayers to Huh7 cells was evaluated using a cytotoxicity detection kit (Roche, Mannheim, Germany). This method was used to quantify the release of lactate dehydrogenase (LDH) into the culture medium, serves as an indicator of cell damage. The procedure was performed according to the manufacturer's protocol. Culture medium collected at each time point was incubated with the reaction mixture from the kit and assessed by a multimode microplate reader (BioTek Instruments, USA) and read at an absorbance of 490 nm with a reference wavelength of 630 nm.

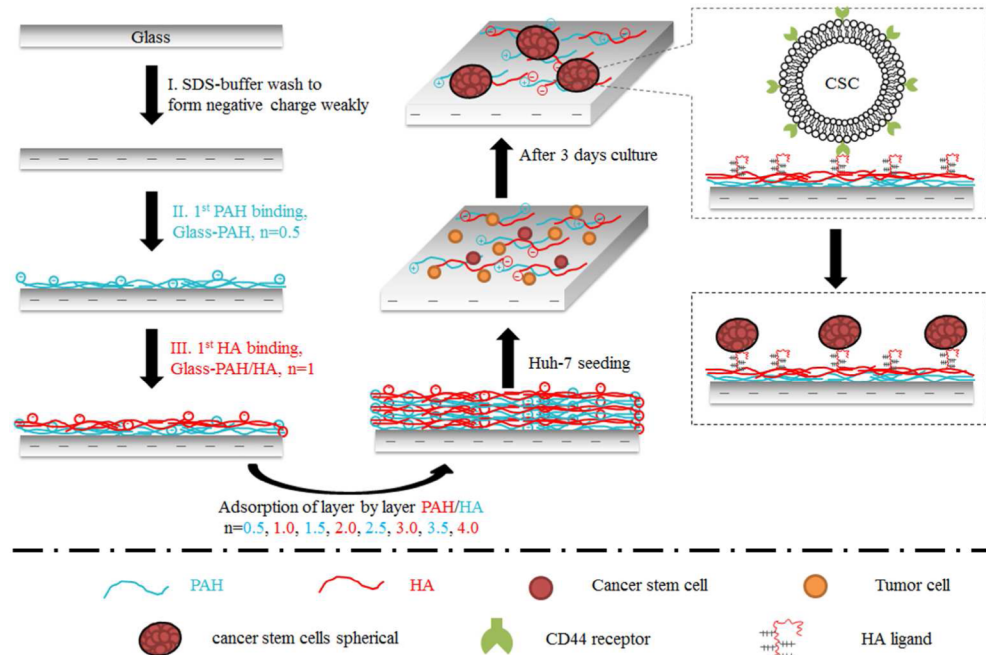
Live and Dead Assay. The viability of Huh7 cells on different substrates and a TCPS control was determined by fluorescence-based live and dead assays (LIVE/DEAD kit, Life, USA). After 3 and 7 days of culture, 100 μL of the dye was mixed with 100 μL of the retained medium, added to each well and incubated at 37 °C for 15 min. After 15 min of incubation, images of live (green) and dead (red) cells were captured using a fluorescence microscope equipped with a digital camera (ECLIPSE-TS100, Nikon, USA).

Cell Viability Assay. Cell viability was evaluated at each time point using MTT reagent, 3-(4,5-cimethylthiazol-2-yl)-2,5-diphenyl tetrazolium bromide, as described in a previous study, with some modifications.²⁸ The MTT (M-2128, Sigma, St. Louis, MO, USA) solution was prepared as a 5 mg/mL stock solution in PBS, sterilized by Millipore filtration, and then kept in the dark. After culture, the medium was discarded, and 200 μL of the MTT solution was added to each well, kept at 37 °C and incubated for 3 h. Then, the solution was removed and 200 μL of dimethyl sulfoxide (Sigma, USA) was added to dissolve the formazan crystals. The optical density of the formazan solution was read by a multimode microplate reader (BioTek Instruments, USA) at 570 nm. The OD values were also fitted to a standard curve.

CSCs Surface Marker Analysis by Flow Cytometry Analysis. Cell surface marker analysis is widely used in CSC selection, particularly a double immunofluorescence staining technique for the detection of two CSC markers by flow cytometry analysis. Cells isolated from (PAH/HA)₁, (PAH/HA)₂, (PAH/HA)₃, and a TCPS substrate as a control group were analyzed. Cells were detached by 0.2% (w/v) trypsin and single cell suspension obtained by passing cells through the mesh. The following antibodies were used to stain cells: FITC-conjugated anti-CD44 (BD Pharmingen, USA) and phycoerythrin (PE)-conjugated anti-CD133/2 (Miltenyi biotec, Bergisch Gladbach, Germany). Cells were analyzed using a FACScan flow cytometer (Becton Dickinson, San Jose, CA, USA), and data were acquired using Cellquest software. The presence or absence of staining was compared with the appropriate isotype control.

Chemoresistance Test. To determine the drug sensitivity of the cells isolated from PAH/HA multilayer films, Huh7 cells isolated from (PAH/HA)₂, (PAH/HA)₃, and the TCPS control group were determined. Cells were seeding at the density of 3 × 10⁴ cells/mL, incubated at 37 °C for 3 days. Then, cells were changed with the medium mixing with doxorubicin (MW = 579.98, Sigma, USA), a kind

Scheme 1. Schematic Illustrations (Not to Scale) of Layer-by-Layer PAH/HA Multilayer Film Formation, Huh7 Cell Seeding, and CSC Colony Formation^a



^aCSCs semi-attached on the surface and formed colonies after 3 days of culture. The proposed mechanism of the colony–HA interaction is also depicted.

of clinical chemotherapeutic agent on HCC, ranging from the concentration gradient of 0 to 20 $\mu\text{g mL}^{-1}$. Cell viability was evaluated by MTT assay after 3 days and 7 days incubation. The OD values were fitted into cell number and the relative viability with the drug concentration gradient were analyzed. Especially, IC₅₀ of Huh7 cell on TCPS was also calculated.

Real-Time Quantitative Reverse Transcriptase Polymerase Chain Reaction (RT-PCR). Total cellular RNA was extracted by using RNA extraction kit (RNA Mini Kit, Applied Biosystems, USA). The cDNA synthesis was performed according to the manufacturer's instructions from RNA isolation from cells (Applied Biosystems, USA). Real-Time PCR System Thermal Cycling Block (Applied Biosystems, USA) was performed and monitored the gene expressions in real time. The level of expression of each target gene was normalized to the reference gene glyceraldehyde phosphate dehydrogenase (GAPDH) and the resulting data were expressed as a ratio of the control. Data were collected with instrument spectral compensations by the Applied Biosystems StepOne Software v2.2.2, and analyzed using the threshold cycle number (Ct) relative quantification method. The Albumin, G6P, GAPDH, Nanog, Oct4 and Sox2 were detected by the SYBR Green Real-Time PCR with the predesigned assays (Assay ID: NM_000477.5, NM_000151.2, NM_002046.3, NM_024865.2, NM_002701.4, NM_003106.2, Applied Biosystems, USA).

Statistical Analysis. All data were expressed as mean values \pm error. Six independent specimens were determined and each experiment was repeated at least 2 times. Student's *t* test was used for evaluating statistical significance and was indicated as follow: **P* < 0.05, ***P* < 0.01, ****P* < 0.005, and *****P* < 0.0001.

RESULTS AND DISCUSSION

The layer-by-layer adsorption of PAH/HA multilayer films is illustrated in Scheme 1. The formation of PEM films was achieved through the electrostatic interaction of PAH as a polycation and HA as a polyanion. After the fabrication of the PAH/HA multilayer films, Huh7 cells were seeded sequentially on the substrates and the TCPS control group.

Monitoring of PAH/HA Multilayer Film Buildup by Quartz Crystal Microbalance. Figure 1 shows the QCM

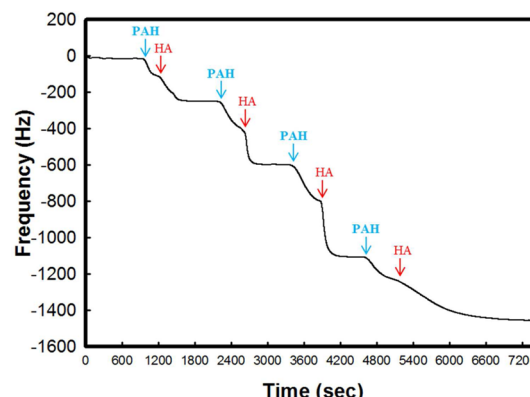


Figure 1. QCM analysis of layer-by-layer adsorption of PAH/HA multilayer films. PAH solution (blue) was injected into the QCM chamber and adsorbed on a Au chip, giving rise to a dipole–dipole interaction, followed by the injection of HA solution (red) and the layer-by-layer adsorption of up to 4 layers.

profiles for the formation of PAH/HA multilayer films and illustrates the characteristics of the layer-by-layer adsorption. QCM data shows the substances deposited on the Au surface may not provide the exact thickness in comparison with that on glass. Therefore, herein, the QCM data could only provide the layer by layer deposition procedure and fabrication feasibility of the multilayer films. The quality of the PAH/HA multilayer films buildup was assessed by monitoring the variation in frequency. The PEM films were built up by the adsorption of PAH on the Au chip after treating with O₂ plasma. HA adsorption then formed a (PAH/HA)₁ substrate. The layer-by-

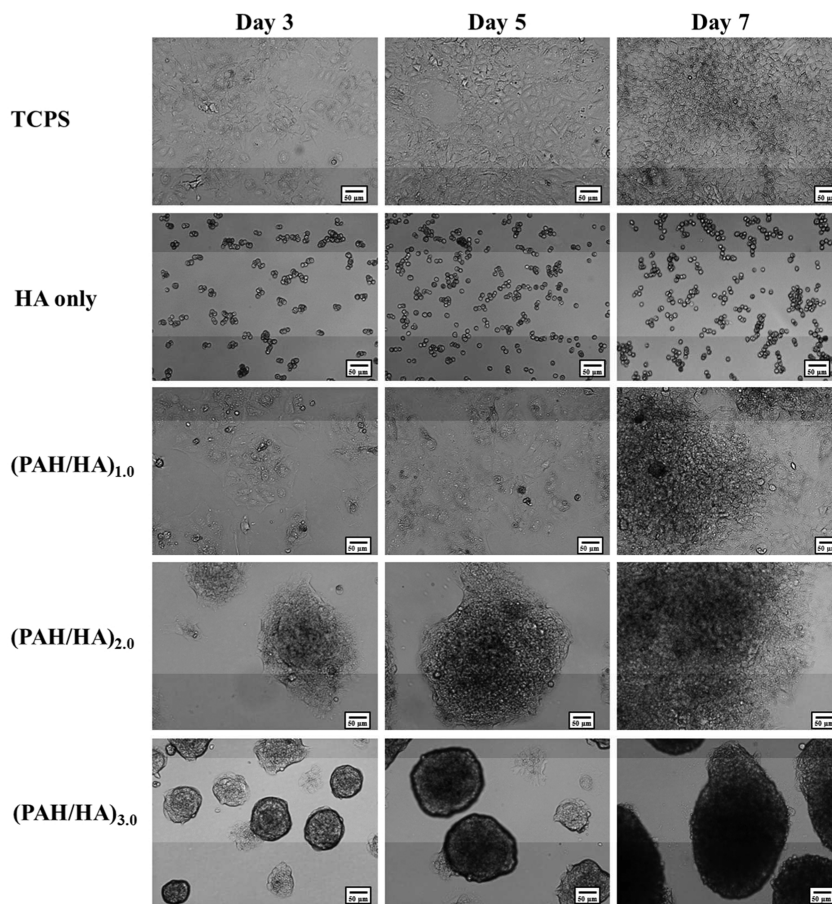


Figure 2. Morphological examination of Huh7 cells seeded on TCPS, HA coating on TCPS, $(\text{PAH}/\text{HA})_1$, $(\text{PAH}/\text{HA})_2$, and $(\text{PAH}/\text{HA})_3$ by optical phase contrast microscopy after 3, 5, and 7 days of culture.

layer adsorption shown in the QCM profile in Figure 1(A) corresponds to steps (II–III) shown in Scheme 1. It is shown that the frequency decreased during the layer-by-layer adsorption step and the Δf decrease became larger as the number of layers increased up to 3 layers, especially when the HA solution was added. The Δf means the total mass originated from the sum of layer and trapped water; the larger Δf revealed that the more mass adsorbed on the substrate. It is suggested that the layer of HA may trapped more amount of water than that of PAH layer which resulted in larger Δf variation. However, the variation in frequency decreased, become smooth after layer 4. It is suggested that the adsorption mass decreased after the deposition of 3–4 layers and resulted a smaller Δf variation and resulted in the smooth curve. In addition, S1 demonstrated the zeta potential measurement of PAH/HA multilayer films to monitor the charge accumulation approached surfaces. As shown in S1, all PAH-ending multilayer films displayed more relative positive zeta potential, and all HA-ending multilayer films exhibited more relative negative zeta potential. Furthermore, the relative values of each layer variation were decreased as the number of the layer increased. The absolute values of the zeta potential reaching a plateau as the layer increased up to 3 which means the surface charge approach charge neutrality as the number of the layer increased. Therefore, combined with QCM data, the adsorption mass decreased after the deposition overtook 3 layers due to the charge neutrality of the surface which resulted in the smooth curve of Δf variation.

Colony Formation on HA Only Surface and PAH/HA Multilayer Films. Since clinical cancer tissue specimens are significantly more complex than cell lines, herein, the Huh7 cell line, one of the commonly utilized HCC cell lines originally taken from a liver tumor was used in this study as the model cell to model cancer stem cell environment and to select and enrich the stem cell-like cells. The cell morphology and colony formation on the HA-coated substrate and PAH/HA multilayer films were investigated (Figure 2). The cells displayed single but not spread out morphologies on the HA-coated surfaces, which were very different from the morphology observed on the TCPS substrate. In contrast, cell aggregation increased as the number of layers increased and formed colonies on the films with an HA end-layer. Cells were spread out on $(\text{PAH}/\text{HA})_1$ and displayed some clustering on $(\text{PAH}/\text{HA})_2$. Furthermore, colony formation was observed when Huh7 cells were seeded on $(\text{PAH}/\text{HA})_3$ after 3 days of culture, and these colonies became larger with increasing culture time. In particular, after 7 days of culture, the size of some colonies was increased to $200 \mu\text{m}$ in diameter, and the boundaries of the colonies were very clear. The results suggest that the colonies formed on $(\text{PAH}/\text{HA})_3$ may have displayed the ability to grow become enriched.

Cell Viability Assay. The cytotoxicity and cell viability of Huh7 cells on PAH/HA multilayer films were evaluated by an MTT assay, a lactate dehydrogenase (LDH) assay, and a live/dead assay. Figure 3(A) shows the MTT assay of Huh7 cells cultured on PAH/HA multilayer films, with the OD values

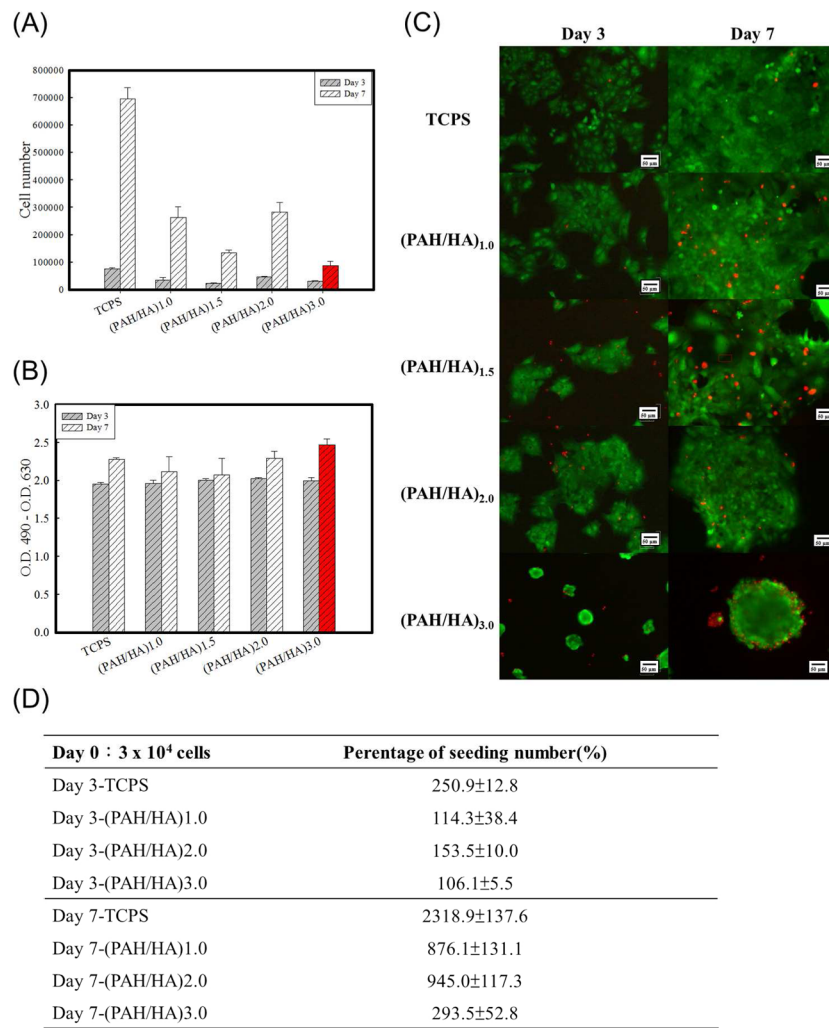


Figure 3. (A) Cell viability assay of Huh7 cells seeded on TCPS and PEMs after 3 and 7 days of culture. (B) LDH activity released from Huh7 cells cultured on TCPS, glass and different PEM films after 3 and 7 days of incubation. The optical density of the LDH activity was read on an ELISA plate reader at 490 nm, with a reference wavelength of 630 nm. (C) Live and dead expression of Huh7 cells seeded on TCPS and PEMs after 3 and 7 days culture. (D) Cell number and percentage of seeding number of cells isolated from different culture substrates, TCPS, (PAH/HA)₁, (PAH/HA)_{1.5}, (PAH/HA)₂, and (PAH/HA)₃ after 3 and 7 days of culture.

fitted to the cell number. In addition, cell number and percentage of seeding number of cells isolated from different culture substrates, after 3 and 7 days of culture were summarized in Figure 3(D). The results indicate that the number of cells on the HA end-layers was less than that on the TCPS substrate after 3 days culture, which also indirectly suggests a selection effect. Furthermore, after 7 days of culture, Figure 3(D) revealed that the growth efficiency of PAH/HA multilayer is down regulated as the number of the layer increased. Our previous study also demonstrated that PEM films with a high layer number could be used to facilitate stem-cell-like niches and displayed better efficiency of colony formation than that on PEM films composed of a fewer of layers.²⁹ Furthermore, the increase in cell number on (PAH/HA)₃ was lower than that on (PAH/HA)₁ and (PAH/HA)₂, which suggests that the rate at which the number of cells increased in a three-dimensional environment was lower than that in a two-dimensional environment.

In addition, the cell cytotoxicity of the PAH/HA multilayer films was determined by using an LDH assay. Figure 3B shows that the release of LDH on sequential PAH/HA multilayer films was very similar to that on TCPS, incorporate with the

cell number data, which demonstrate that the dead cell ratio on sequential HA-based substrates is higher than that on TCPS. It is considered that the environment of the HA-based multilayer films may inappropriate for normal cancer cells not form colony to spread and migrate and may more suitable for colony forming cells to live. Furthermore, as shown in Figure 3C, the live/dead assay also revealed that the dead cells on the HA-based multilayer films were investigated around the boundary of the colonies and the number was a little higher than that on TCPS substrate which was consistent with Figure 3B.

Marker Expressions of Huh7 Colonies Cells Selected from (PAH/HA)₃. Currently, there is no apparent consensus regarding the “best marker(s)” or “single marker” that can be used for the identification of CSCs in any cancer as well as HCC. However, to elucidate whether selected cell colonies from (PAH/HA)₃ could be enriched cells expressing putative cancer stem cell markers, the expression profile of the two representative HCC cancer stem cell surface markers CD133 and CD44 were used to assay immunophenotype expressions.^{5,7} The percentages of double positive cells on these multilayer films are illustrated in Figure 4A, and the data obtained from two independent experiments are shown in

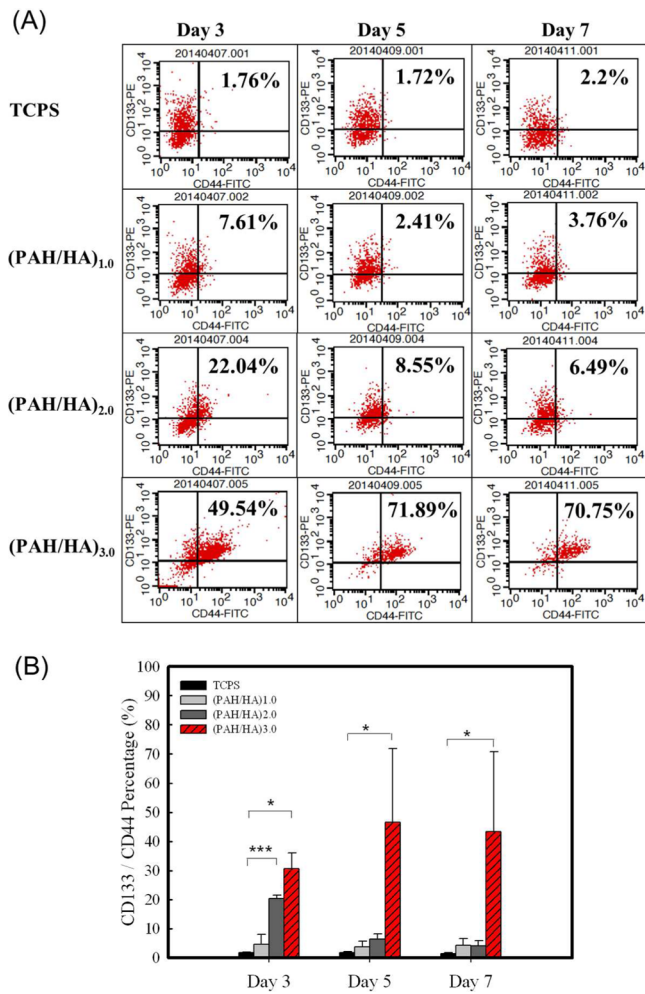


Figure 4. (A) Flow cytometry analysis and percentages of double positive expression for CD133/CD44 of Huh7 cells isolated from TSPC, $(\text{PAH}/\text{HA})_1$, $(\text{PAH}/\text{HA})_2$, and $(\text{PAH}/\text{HA})_3$ after 3, 5, and 7 days of culture. (B) Histogram of the percentage of double positive expression cells isolated from TCPS and a series of PAH/HA multilayer films determined by independent experiments. Asterisks denote significant differences in the percentage of $\text{CD}133^+/\text{CD}44^+$ expression (* $p < 0.05$ and *** $p < 0.005$) as determined by a Student's *t* test.

Figure 4B. The percentage of $\text{CD}133^+/\text{CD}44^+$ double positive cells isolated from TCPS was consistently lower than 5% at each time point. In contrast, the percentage of $\text{CD}133^+/\text{CD}44^+$ double positive cells increased as the number of layers increased after 3 days of culture. The percentage was approximately 7.61% on the $(\text{PAH}/\text{HA})_1$ film and 50% on the $(\text{PAH}/\text{HA})_3$ film. Huh7 cells replicated continuously with a doubling time of 47–51 h and the MTT assay of day 3 reflected the cell numbers after 1–2 doubling, however, the result of cell viability assay demonstrated the cell number of $(\text{PAH}/\text{HA})_3$ was only 100% of the seeding number after 3 days of culture which was lower than all of the other substrates and was suggested that due to the selection effect. Combined the MTT assay and the marker expression, it is considered that $(\text{PAH}/\text{HA})_3$ provide a better microenvironment for CSCs selection when compared with $(\text{PAH}/\text{HA})_1$ and $(\text{PAH}/\text{HA})_2$ substrates. Furthermore, the percentages of double positive cells on the $(\text{PAH}/\text{HA})_1$ and $(\text{PAH}/\text{HA})_2$ films all decreased after 7 days of culture and were similar to the percentage of such cells on TCPS. It is suggested

that although cell aggregation could be observed on $(\text{PAH}/\text{HA})_1$ and $(\text{PAH}/\text{HA})_2$ during an earlier culture stage, these aggregated cells attached and migrated from the cluster, and the colony type could not be maintained after long-term culture. This phenomenon is consistent with the results obtained regarding cell morphology, as shown in Figure 2. In contrast, the percentage of double positive cells on $(\text{PAH}/\text{HA})_3$ increased with culture time and reached up to 70% after 7 days of culture. This result is also consistent with the concept of colony selection. In our previous study, PLL/PLGA polypeptide films have been used to select liver stem cells and we also found that the few layers of negative ending polypeptide films appear to display excellent ability of selection but less capable of maintaining of stem cell colony.²⁹ It is considered that the hardness of the underneath of glass may affect the mechanical properties especially under fewer layers. In addition, the water adsorption led to softer films of the higher layer may also assist the colony maintenance. As shown in Figure S2, the morphological investigation of Huh7 cells seeded on different concentration of PAH/HA multilayer films after 3 days of culture were observed. It is showed that fewer layers were needed to form colony as the polyelectrolyte material concentration increased which is also consistent with the hypothesis of softness effect. HA is not only a key extracellular matrix of stem cells and CSCs niches but also functions as a bioregulatory molecule.¹⁸ HA concentrations are suggested to be typically higher in malignant tumors than in normal tissue.¹⁶ Besides, HA/CD44 interactions promote retention of surrounding cellular matrix and regulate many intracellular signaling pathways which influence multiple cellular functions includes stem cell self-renewing and homing.¹⁵ Previous studies have also revealed that overexpression of CD44 has been shown to be closely associated with breast tumor, head and neck carcinoma cells growth, migration, and invasion.^{30,31} Herein, HA-based multilayer films provided a series of microenvironment variations to modulate cancer cell behavior and the $(\text{PAH}/\text{HA})_3$ films provided a suitable niche for colony formation and enrichment. The results demonstrate that the selection and enrichment of CSCs can be regulated by modulating surface properties.

Drug-Resistance Assay: Doxorubicin. To access the drug resistance of selected colonies from the $(\text{PAH}/\text{HA})_3$ film, an MTT assay was used to determine cell viability and assay chemotherapeutic drug-induced apoptosis. Huh7 cells cultured on TCPS, $(\text{PAH}/\text{HA})_2$, and $(\text{PAH}/\text{HA})_3$ substrates were treated with gradient concentrations of doxorubicin after 3 days culture. Curves showing the variation in relative viability with the drug concentration gradient after 3 days and 7 days of incubation are shown in Figure 5A and 5B, respectively. The relative cell viability on the $(\text{PAH}/\text{HA})_2$ film decreased as the doxorubicin concentration increased, which is similar to the behavior observed on the TCPS substrate. In the literature, the IC_{50} of doxorubicin has been reported to be approximately 1 μM . In this study, the IC_{50} of doxorubicin on the TCPS substrate was also observed to be approximately 1 μM . In contrast, the relative viability of Huh7 cells on the $(\text{PAH}/\text{HA})_3$ film showed a significant variation as the doxorubicin concentration increased (** $p < 0.005$ for 10 μM and **** $p < 0.001$ for 20 μM) after 3 days of incubation (Figure 4A). Furthermore, the cell viabilities of Huh7 cells on TCPS and $(\text{PAH}/\text{HA})_3$ after 7 days of incubation were similar to those observed after 3 days of incubation, but the cells on the $(\text{PAH}/\text{HA})_3$ film displayed very high drug resistance over the

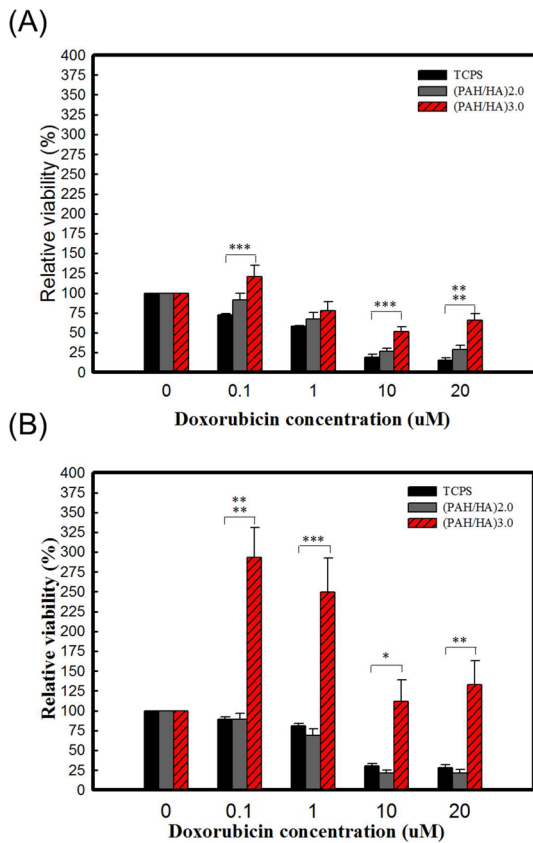


Figure 5. Drug resistance test of the Huh7 cells cultured on TCPS, (PAH/HA)₂ and (PAH/HA)₃ incubated with doxorubicin in gradient concentrations after (A) 3 and (B) 7 days of culture. The relative cell viabilities of different substrates at various concentrations of doxorubicin were determined by an MTT assay. Asterisks denote significant differences in the relative viability after treatment with doxorubicin (* $p < 0.05$, ** $p < 0.01$, *** $p < 0.005$, **** $p < 0.001$) as determined by a Student's *t* test.

concentration range from 0.1 μM to 20 μM . Although the relative viability decreased as the drug concentration increased, it was observed that these selected colonies not only survived but were also enriched after 7 days of incubation. Figure 3D have also demonstrated the cell number on (PAH/HA)₃ increased with culture periods. The results of a drug resistance assay are also consistent with the marker expressions of CSCs. Therefore, the cell number increased and the CSCs properties were enhanced after 7 days culture on (PAH/HA)₃ which revealed that the CSCs were enriched on (PAH/HA)₃ multilayer films. It is concluded that the (PAH/HA)₃ provided a colony formation niche and enhanced the enrichment of CSCs over time. In addition, as shown in Figure 5B, the relative viability of Huh7 cells on (PAH/HA)₃ increased by up to 300% and 250% when the drug concentration was 0.1 μM and 1 μM , respectively, which suggests that the low-concentration drug treatment could not induce cell apoptosis but did stimulate CSC proliferation.

Gene Expression. To further confirm the stem cell-like characteristics of the cells examined, the expression levels of three stem cell markers (i.e., Nanog, Sox2, and Oct4) and two mature hepatocyte markers (G6P and Albumin) in Huh7 cells isolated from (PAH/HA)₃ after 3 days and 7 days of culture were evaluated, and the corresponding expression levels were normalized by the expression of Huh7 cells on TCPS. As

shown in Figure 6, the results indicate that G6P and albumin were all detected and that the expression levels were similar to

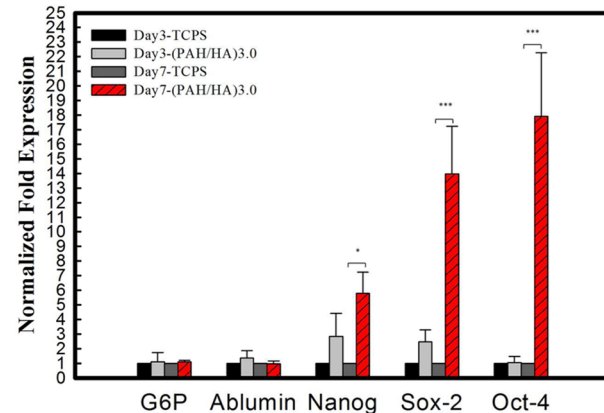


Figure 6. Gene expression of Huh7 cells cultured on (PAH/HA)₃ and TCPS substrate after 7 days of culture. G6P and albumin were mature liver cell genes. Nanog, Sox-2, and Oct-4 were stem-cell-like genes. Asterisks denote significant differences in gene expression relative to that of a control (* $p < 0.05$, *** $p < 0.005$) as determined by a Student's *t* test.

those observed on TCPS. In contrast, the stem cell marker expression of cells on (PAH/HA)₃ was slightly higher than that of cells on TCPS after 3 days of culture. Furthermore, after 7 days of culture, the expression levels of stem-cell-related genes all increased significantly. In comparing the expression levels of various markers with the expression level observed on TCPS, the following results were observed: 5.8-fold for Nanog gene (* $p < 0.05$), 14-fold for Sox 2 (** $p < 0.005$), and 17.9-fold for Oct4 (** $p < 0.005$). Shan et al. demonstrated that Nanog expression was positively correlated with vascular and capsular invasion and also indicated that Nanog-positive cells might exhibit stem-cell-like characteristics in HCC.²⁶ The authors also used Nanog as a marker to sort Nanog^{High} cells and demonstrated that increased levels of Nanog, Oct4, and Sox2 were present in sorted Nanog^{High} cells compared with Nanog^{Low} cells, which is also consistent with our results. It is concluded that the gene expression results confirm our speculation and demonstrate that colonies isolated from the (PAH/HA)₃ substrate may have displayed stem-cell-like characteristics.

CONCLUSIONS

Taken together, the results of this study indicate that the HA-based multilayer films created allowed for surface variation for the fabrication of cancer stem cell niches. Colony formation could be observed on the (PAH/HA)₃ film, and these colonies displayed a stem-cell-like phenotype, a high percentage of CSC marker expression in HCC cells, surprising chemo-resistance and high levels of stem cell gene expression. This system allows for label-free selection and enrichment on CSCs by surface niches mimicking and also provides a useful platform for drug screening in cancer therapy.

ASSOCIATED CONTENT

Supporting Information

The Supporting Information is available free of charge on the ACS Publications website at DOI: 10.1021/acsami.5b04436.

Zeta potential measurement of PAH/HA multilayer films and coating concentration gradient tested of Huh 7 cells on PAH/HA PEM films. ([PDF](#))

AUTHOR INFORMATION

Corresponding Author

*E-mail: iclee@mail.cgu.edu.tw. Tel.: +886-3-2118800 ext 5985.

Notes

The authors declare no competing financial interest.

ACKNOWLEDGMENTS

Funding for this work was provided by Chang Gung University and by grants awarded through the National Science Council Taiwan (grants NSC 102-2221-E-182-007 and MOST 103-2221-E-182-011 to I-C.L.). We also gratefully acknowledge the cell line provided by Chia-Ning Shen (Genomics research center, Academia Sinica) and the support provided in operating the QCM instrument by Professor Chii-Wann Lin (National Taiwan University).

REFERENCES

- (1) Visvader, J. E.; Lindeman, G. J. Cancer Stem Cells in Solid Tumours: Accumulating Evidence and Unresolved Questions. *Nat. Rev. Cancer* **2008**, *8*, 755–768.
- (2) Lapidot, T.; Sirard, C.; Vormoor, J.; Murdoch, B.; Hoang, T.; Caceres-Cortes, J.; Minden, M.; Paterson, B.; Caligiuri, M. A.; Dick, J. E. A Cell Initiating Human Acute Myeloid Leukaemia after Transplantation into SCID Mice. *Nature* **1994**, *367*, 645–648.
- (3) Trumpp, A.; Wiestler, O. D. Mechanisms of Disease: Cancer Stem Cells—Targeting the Evil Twin. *Nat. Clin. Pract. Oncol.* **2008**, *5*, 337–347.
- (4) Llovet, J. M.; Burroughs, A.; Bruix, J. Hepatocellular Carcinoma. *Lancet* **2003**, *362*, 1907–1917.
- (5) Feng, D.; Wang, N.; Hu, J.; Li, W. Surface Markers of Hepatocellular Cancer Stem Cells and Their Clinical Potential. *Neoplasma* **2014**, *61*, 505–513.
- (6) Ma, S.; Chan, K. W.; Hu, L.; Lee, T. K.; Wo, J. Y.; Ng, I. O.; Zheng, B. J.; Guan, X. Y. Identification and Characterization of Tumorigenic Liver Cancer Stem/Progenitor Cells. *Gastroenterology* **2007**, *132*, 2542–2556.
- (7) Zhu, Z.; Hao, X.; Yan, M.; Yao, M.; Ge, C.; Gu, J.; Li, J. Cancer Stem/Progenitor Cells are Highly Enriched in CD133+CD44+ Population in Hepatocellular Carcinoma. *Int. J. Cancer* **2010**, *126*, 2067–2078.
- (8) Hadnagy, A.; Gaboury, L.; Beaulieu, R.; Balicki, D. SP Analysis may be Used to Identify Cancer Stem Cell Populations. *Exp. Cell Res.* **2006**, *312*, 3701–3710.
- (9) Mihatsch, J.; Toulany, M.; Bareiss, P. M.; Grimm, S.; Lengerke, C.; Kehlbach, R.; Rodemann, H. P. Selection of Radioresistant Tumor Cells and Presence of ALDH1 Activity in Vitro. *Radiat. Oncol.* **2011**, *99*, 300–306.
- (10) Haraguchi, N.; Utsunomiya, T.; Inoue, H.; Tanaka, F.; Mimori, K.; Barnard, G. F.; Mori, M. Characterization of a Side Population of Cancer Cells from Human Gastrointestinal System. *Stem Cells* **2006**, *24*, 506–513.
- (11) Salnikov, A. V.; Kusumawidjaja, G.; Rausch, V.; Bruns, H.; Gross, W.; Khamidjanov, A.; Ryschich, E.; Gebhard, M. M.; Moldenhauer, G.; Buchler, M. W.; Schemmer, P.; Herr, I. Cancer Stem Cell Marker Expression in Hepatocellular Carcinoma and Liver Metastases is not Sufficient as Single Prognostic Parameter. *Cancer Lett.* **2009**, *275*, 185–193.
- (12) Facchino, S.; Abdouh, M.; Chatoo, W.; Bernier, G. BMI1 Confers Radioresistance to Normal and Cancerous Neural Stem Cells through Recruitment of the DNA Damage Response Machinery. *J. Neurosci.* **2010**, *30*, 10096–10111.
- (13) Ye, J.; Wu, D.; Wu, P.; Chen, Z.; Huang, J. The Cancer Stem Cell Niche: Cross Talk between Cancer Stem Cells and their Microenvironment. *Tumor Biol.* **2014**, *35*, 3945–3951.
- (14) Yi, S. Y.; Hao, Y. B.; Nan, K. J.; Fan, T. L. Cancer Stem Cells Niche: a Target for Novel Cancer Therapeutics. *Cancer Treat. Rev.* **2013**, *39*, 290–296.
- (15) Williams, K.; Motiani, K.; Giridhar, P. V.; Kasper, S. CD44 Integrates Signaling in Normal Stem Cell, Cancer Stem Cell and (Pre)metastatic Niches. *Exp. Biol. Med.* **2013**, *238*, 324–338.
- (16) Jiang, D.; Liang, J.; Noble, P. W. Hyaluronan in Tissue Injury and Repair. *Annu. Rev. Cell Dev. Biol.* **2007**, *23*, 435–461.
- (17) Endo, K.; Terada, T. Protein Expression of CD44 (standard and variant isoforms) in Hepatocellular Carcinoma: Relationships with Tumor Grade, Clinicopathologic Parameters, p53 Expression, and Patient Survival. *J. Hepatol.* **2000**, *32*, 78–84.
- (18) Bourguignon, L. Y. Hyaluronan-CD44 Interaction Promotes microRNA Signaling and RhoGTPase Activation Leading to Tumor Progression. *Small GTPases* **2012**, *3*, 53–59.
- (19) Bourguignon, L. Y.; Shiina, M.; Li, J. J. Hyaluronan-CD44 Interaction Promotes Oncogenic Signaling, microRNA Functions, Chemoresistance, and Radiation Resistance in Cancer Stem Cells Leading to Tumor Progression. *Adv. Cancer Res.* **2014**, *123*, 255–275.
- (20) Singh, S. K.; Clarke, I. D.; Terasaki, M.; Bonn, V. E.; Hawkins, C.; Squire, J.; Dirks, P. B. Identification of a Cancer Stem Cell in Human Brain Tumors. *Cancer Res.* **2003**, *63*, 5821–5828.
- (21) Ponti, D.; Costa, A.; Zaffaroni, N.; Pratesi, G.; Petrangolini, G.; Coradini, D.; Pilotti, S.; Pierotti, M. A.; Daidone, M. G. Isolation and In vitro Propagation of Tumorigenic Breast Cancer Cells with Stem/Progenitor Cell Properties. *Cancer Res.* **2005**, *65*, 5506–5511.
- (22) Qiu, X.; Wang, Z.; Li, Y.; Miao, Y.; Ren, Y.; Luan, Y. Characterization of Sphere-forming Cells with Stem-like Properties from the Small Cell Lung Cancer Cell Line H446. *Cancer Lett.* **2012**, *323*, 161–170.
- (23) Chiou, S. H.; Wang, M. L.; Chou, Y. T.; Chen, C. J.; Hong, C. F.; Hsieh, W. J.; Chang, H. T.; Chen, Y. S.; Lin, T. W.; Hsu, H. S.; Wu, C. W. Coexpression of Oct4 and Nanog Enhances Malignancy in Lung Adenocarcinoma by Inducing Cancer Stem Cell-Like Properties and Epithelial-Mesenchymal Transdifferentiation. *Cancer Res.* **2010**, *70*, 10433–10444.
- (24) Ma, B.; Lei, X.; Guan, Y.; Mou, L. S.; Yuan, Y. F.; Yue, H.; Lu, Y.; Xu, G. T.; Qian, J. Maintenance of Retinal Cancer Stem Cell-Like Properties through Long-Term Serum-Free Culture from Human Retinoblastoma. *Oncol. Rep.* **2011**, *26*, 135–143.
- (25) Lee, I. C.; Liu, Y. C.; Tsai, H. A.; Shen, C. N.; Chang, Y. C. Promoting the Selection and Maintenance of Fetal Liver Stem/Progenitor Cell Colonies by Layer-by-Layer Polypeptide Tethered Supported Lipid Bilayer. *ACS Appl. Mater. Interfaces* **2014**, *6*, 20654–20663.
- (26) Shan, J.; Shen, J.; Liu, L.; Xia, F.; Xu, C.; Duan, G.; Xu, Y.; Ma, Q.; Yang, Z.; Zhang, Q.; Ma, L.; Liu, J.; Xu, S.; Yan, X.; Bie, P.; Cui, Y.; Bian, X. W.; Qian, C. Nanog Regulates Self-Renewal of Cancer Stem Cells through the Insulin-Like Growth Factor Pathway in Human Hepatocellular Carcinoma. *Hepatology* **2012**, *56*, 1004–1014.
- (27) Lee, I. C.; Wu, Y. C. Facilitating Neural Stem/Progenitor Cell Niche Calibration for Neural Lineage Differentiation by Polyelectrolyte Multilayer Films. *Colloids Surf., B* **2014**, *121*, 54–65.
- (28) Lee, I. C.; Lee, Y. T.; Yu, B. Y.; Lai, J. Y.; Young, T. H. The Behavior of Mesenchymal Stem Cells on Micropatterned PLLA Membranes. *J. Biomed. Mater. Res., Part A* **2009**, *91*, 929–938.
- (29) Tsai, H. A.; Wu, R. R.; Lee, I. C.; Chang, H. Y.; Shen, C. N.; Chang, Y. C. Selection, Enrichment, and Maintenance of Self-Renewal Liver Stem/Progenitor Cells Utilizing Polypeptide Polyelectrolyte Multilayer Films. *Biomacromolecules* **2010**, *11*, 994–1001.
- (30) Bourguignon, L. Y. Hyaluronan-Mediated CD44 Activation of RhoGTPase Signaling and Cytoskeleton Function Promotes Tumor Progression. *Semin. Cancer Biol.* **2008**, *18*, 251–259.
- (31) Wang, S. J.; Bourguignon, L. Y. Role of Hyaluronan-Mediated CD44 Signaling in Head and Neck Squamous Cell Carcinoma Progression and Chemoresistance. *Am. J. Pathol.* **2011**, *178*, 956–963.